LETTER

Synthesis and crystal structure of $Li_{0.52}Mg_{0.96}Sc_{0.52}Si_2O_6$ orthopyroxene

HEXIONG YANG* AND ROBERT T. DOWNS

Department of Geosciences, University of Arizona, Tucson, Arizona 85721-0077, U.S.A.

ABSTRACT

$Li_{0.52}Mg_{0.96}Sc_{0.52}Si_2O_6$ orthopyroxene was synthesized by the flux method and its structure studied with single-crystal X-ray diffraction. The crystal is orthorhombic with space group *Pbca* and unit-cell parameters $a = 18.259(5)$, b = 8.883(2), c = 5.271(1) Å, and $V = 854.9(3)$ Å^3. The structure refinement shows that the M1 and M2 sites are occupied by (0.48 Mg + 0.52 Sc) and (0.48 Mg + 0.52 Li), respectively. While the O3-O3-O3 kinking angle (165.40°) of the silicate tetrahedral A chain appears to be normal when compared with reported data, the kinking angle (151.92°) of the B chain is the largest of all orthopyroxenes examined at ambient conditions. This is the first orthopyroxene structure that contains more than 50% trivalent and monovalent cations in the M1 and M2 sites, respectively, and displays a kinking angle of the tetrahedral B chain that is greater than 150°. Our study demonstrates the stability of the new pyroxene structure type predicted by Pannhorst (1979) at room temperature.

Keywords: $Li_{0.52}Mg_{0.96}Sc_{0.52}Si_2O_6$, orthopyroxene, crystal structure, X-ray diffraction

INTRODUCTION

Magnesium-bearing silicate pyroxene is a common rock-forming mineral in the Earth's crust and upper mantle, as well as meteorites, and a major component of steatite ceramics. It may occur in one of the following four structural symmetries: *Pbcn* protopyroxene, *Pbca* orthopyroxene, $P2_1/c$ clinopyroxene, and *C2/c* clinopyroxene (see review by Cameron and Papike 1981). The relative stabilities, structural relationships, and phase transformation mechanisms among these polymorphs, therefore, have been the central subject of numerous investigations in terms of temperature, pressure, and chemical composition. Ito and Steele (1976) conducted the first phase-equilibrium study in the $MgSiO_3$-$LiScSi_2O_6$ join and found four pyroxene polymorphs at 1250 °C. The solid solution of clinopyroxene extends from $LiScSi_2O_6$ (*C2/c*) to $Li_{0.6}Mg_{0.8}Sc_{0.6}Si_2O_6$ ($P2_1/c$). The orthopyroxene solid solution exists at around $Li_{0.5}Mg_{1.0}Sc_{0.5}Si_2O_6$, whereas the protopyroxene solid solution may range from $Li_{0.35}Mg_{1.3}Sc_{0.35}Si_2O_6$ to $MgSiO_3$ (enstatite), but it is non-quenchable if the $MgSiO_3$ content is greater than 90 mol%. A more detailed phase diagram of the $MgSiO_3$-$LiScSi_2O_6$ system was presented by Takéuchi et al. (1984a, 1984b, 1984c), which also includes a new series of clinopyroxene-based superstructures between 1385 and 1550 °C.

The crystal structure of *C2/c* $LiScSi_2O_6$ clinopyroxene was examined by Hawthorne and Grundy (1977), which was found to transform to the $P2_1/c$ symmetry between 0.3 and 0.6 GPa (Arlt and Angel 2000). Smyth and Ito (1977) determined the structure of $Li_{0.30}Mg_{1.4}Sc_{0.30}Si_2O_6$ protopyroxene and confirmed its space group of *Pbcn*, rather than $P2_1cn$, $Pb2n$, or $Pbc2_1$. The structural behavior of $(Li_{0.2}Mg_{1.4}Sc_{0.2}Co_{0.2})Si_2O_6$ protopyroxene at high temperatures was investigated by Murakami et al. (1985) and that of $Li_{0.23}Mg_{1.54}Sc_{0.23}Si_2O_6$ protopyroxene at high pressures by Yang et al. (1999). However, no structure study has yet been performed on Li-Sc-Mg orthopyroxene, though an orthoestatite doped with Li and Fe, $^{M2}(Mg_{0.59}Fe^{2+}_{0.21}Li_{0.20})^{M1}(Mg_{0.74}Fe^{3+}_{0.20}Fe^{2+}_{0.06})Si_2O_6$, was synthesized and studied by Cámara et al. (2006).

The crystal structure of *Pbca* orthopyroxene consists of two symmetrically nonequivalent tetrahedral silicate chains, A and B, and two crystallographically distinct metal sites, denoted M1 and M2 (M = Mg, Fe, Mn, Co, Zn, etc.) (Fig. 1). The octahedrally coordinated M1 site is more regular and, generally, smaller than M2, which has a coordination number varying from 4 to 6, depending on the chemistry (Downs 2003). The cation ordering in orthopyroxene is very pronounced, with smaller and higher valence cations preferring M1 over M2. Both A and B chains running parallel to the c axis are kinked, with the kinking angles φ (= ∠O3-O3-O3) deviating from 180°, the characteristic value for a fully extended chain. In general, the B chain is about 20° more kinked than the A chain at ambient conditions and appears to have a maximum φ angle less than 150°. In this study, we report the synthesis and structure refinement of $Li_{0.52}Mg_{0.96}Sc_{0.52}Si_2O_6$ orthopyroxene, which contains more than 50% trivalent and monovalent cations in the M1 and M2 sites, respectively, and exhibits the most extended kinking angle of the silicate B chain of all orthopyroxene structures determined thus far at ambient conditions.

EXPERIMENTAL PROCEDURES

The crystal used in this study was synthesized by the flux method based on the phase diagram given by Ito (1975). The starting material was a mixture of high purity (99.95%) MgO, SiO_2, Li_2CO_3, and Sc_2O_3 of stoichiometry $Li_{0.5}MgSc_{0.5}Si_2O_6$, which was ground manually under methanol in an agate mortar. The mixture was then placed in a Pt crucible and heated in air in a vertical tube furnace slowly to 600 °C for decarbonation. Following another grinding with K_2WO_4 added as flux (the weight ratio of $Li_{0.5}MgSc_{0.5}Si_2O_6$:$K_2WO_4$ was 1:10), the powder was heated to 1250 °C for 6 h and cooled to 800 °C in ~24 h. After being held at 800 °C for 5 days, the sample was quenched to room temperature. After the dissolution of flux in hot water, most of the final product was found to be small (<0.1 mm) and colorless prismatic crystals. The chemical composition was analyzed with an electron microprobe on three crystals; within the experimental uncertainties, no W or K was detected and all crystals were found to have nearly the starting chemical composition. However, due to the impossibility in accurately analyzing the amount of Li

* E-mail: hyang@geo.arizona.edu

with the electron microprobe, the final composition of the sample was determined by the structure refinement.

Based on optical examination and X-ray diffraction peak profiles, a slightly elongated crystal was selected and mounted on a Bruker Smart CCD X-ray diffractometer equipped with graphite-monochromatized $MoK\alpha$ radiation. Three-dimensional X-ray diffraction data were collected with frame widths of 0.3° in ω and 30 s counting time per frame (see Table 1 for the experimental details). The data were analyzed to locate peaks for the determination of the unit-cell parameters. All reflections were indexed based on an orthorhombic unit cell (Table 1), which was further refined using all observed reflections (global refinement), and corrected for X-ray absorption using the Bruker SADABS program. Observed systematic absences of reflections indicate the unique space group *Pbca*.

The initial structure model for the synthesized Li-Mg-Sc orthopyroxene was taken from that reported by Yang and Ghose (1995a) for orthoenstatite ($Mg_2Si_2O_6$). The structure refinements were performed with the program SHELX97 (Sheldrick

FIGURE 1. Crystal structure of $Li_{0.52}Mg_{0.96}Sc_{0.52}Mg_{0.96}Si_2O_6$ orthopyroxene viewed along *a*.

TABLE 1. Summary of crystal data and refinement results

Structural formula	$(Li_{0.52}Mg_{0.48})(Mg_{0.48}Sc_{0.52})Si_2O_6$
Formula weight (g/mol)	202.50
Crystal size (mm³)	$0.06 \times 0.04 \times 0.03$
Space group	*Pbca* (No. 61)
a (Å)	18.259(4)
b (Å)	8.883(2)
c (Å)	5.271(1)
V (Å³)	854.9(3)
Z	8
ρ_{calc} (g/cm³)	3.146
λ (Å)	0.71069
μ (mm⁻¹)	1.67
θ range for data collection	2.23 to 28.65
No. of reflections collected	6214
No. of independent reflections	1021
No. of reflections with $I > 2\sigma(I)$	753
No. of parameters refined	93
R(int)	0.046
Final *R* factors [$I > 2\sigma(I)$]	$R_1 = 0.033$, $wR_2 = 0.092$
Final *R* factors (all data)	$R_1 = 0.051$, $wR_2 = 0.097$
Goodness-of-fit	1.078

1997) and neutral atomic scattering factors. All atoms were refined with anisotropic displacement parameters. The initial refinements showed that Li was ordered in the M2 site and Sc in M1. Thus, in the subsequent refinements, we assumed full occupations of the M1 site by (Mg + Sc) and M2 by (Mg + Li), and the amount of Li^+ to be equal to that of Sc^{3+} for charge balance. The relative ratios of Mg/Sc in the M1 site and Mg/Li in M2 were allowed to vary, yielding a site occupancy of M1 = [0.517(4) Sc + 0.483 Mg] and M2 = [0.517(4) Li + 0.483 Mg] at the convergence of refinements. Final atomic coordinates and anisotropic displacement parameters are listed in Table 2 and selected bond distances and angles in Table 3.

RESULTS AND DISCUSSION

In $Li_{0.52}Mg_{0.96}Sc_{0.52}Si_2O_6$ orthopyroxene, Li^+ is completely ordered in the M2 site and Sc^{3+} in M1, consistent with previous measurements on various pyroxenes containing Li and/or Sc (Hawthorne and Grundy 1977; Smyth and Ito 1977; Murakami et al. 1985; Ohashi et al. 1978, 1979, 1996; Yang et al. 1999; Redhammer and Roth 2004a, 2004b; Cámara et al. 2006). The resultant structure, therefore, has a crystal-chemical formula of $^{M2}(Li_{0.52}Mg_{0.48})^{M1}(Mg_{0.48}Sc_{0.52})Si_2O_6$ and represents the first orthopyroxene with trivalent and monovalent cations in the M1 and M2 sites, respectively, exceeding 50% of the site occupancies. The previously determined orthopyroxenes containing the most trivalent cations in the M1 site were an orthopyroxene with about 21% $^{M1}Al^{3+}$ (Kosoi et al. 1974) and a synthetic one with 20% $^{M1}Fe^{3+}$ (Cámara et al. 2006).

The most notable structural feature of the $Li_{0.52}Mg_{0.96}Sc_{0.52}Si_2O_6$ orthopyroxene is the value of the kinking angle of its tetrahedral

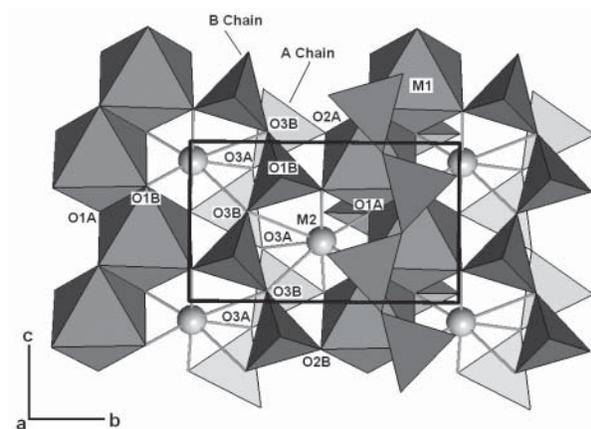**TABLE 3.** Selected bond distances (Å) and angles (°) in $(Mg_{0.48}Li_{0.52})(Mg_{0.48}Sc_{0.52})Si_2O_6$ orthopyroxene

M1-O1A	2.068(2)	SiA-O1A	1.619(2)
M1-O1B	2.079(2)	SiA-O2A	1.590(2)
M1-O1A	2.189(2)	SiA-O3A	1.636(2)
M1-O1B	2.201(2)	SiA-O3A	1.649(2)
M1-O2A	1.995(2)	Avg.	1.624
M1-O2B	2.022(2)	PV	2.178
Avg.	2.092	TAV	22.80
PV	12.039	TQE	1.0057
OAV	33.52		
OQE	1.0111		
M2-O1A	2.118(3)	SiB-O1B	1.626(2)
M2-O1B	2.081(3)	SiB-O2B	1.587(2)
M2-O2A	2.053(3)	SiB-O3B	1.645(2)
M2-O2B	2.033(3)	SiB-O3B	1.646(2)
M2-O3A	2.355(3)	Avg.	1.626
M2-O3B	2.804(3)	PV	2.192
M2-O3B	2.969(3)	TAV	17.166
Avg.	2.345	TQE	1.0044
PV	16.85		
O3A-O3A-O3A	165.40		
O3B-O3B-O3B	151.92		

Notes: PV = Polyhedral volume; OAV = Octahedral angle variance; OQE = Octahedral quadratic elongation; TAV = Tetrahedral angle variance; TQE = Tetrahedral quadratic elongation (Robinson et al. 1971).

TABLE 2. Atomic coordinates and anisotropic displacement parameters for $(Mg_{0.48}Li_{0.52})(Mg_{0.48}Sc_{0.52})Si_2O_6$ orthopyroxene

Atom	x	y	z	U_{eq}	U_{11}	U_{22}	U_{33}	U_{23}	U_{13}	U_{12}
M1	0.3755(1)	0.6482(1)	0.8860(1)	0.0075(3)	0.0072(4)	0.0071(4)	0.0081(4)	−0.0005(3)	−0.0006(3)	−0.0003(3)
M2	0.3745(1)	0.4893(2)	0.3805(4)	0.0164(6)	0.0178(11)	0.0163(12)	0.0152(10)	0.0022(9)	−0.0037(8)	−0.0008(9)
SiA	0.2739(1)	0.3385(1)	0.0629(2)	0.0069(3)	0.0071(5)	0.0068(5)	0.0069(4)	−0.0006(3)	0.0003(3)	−0.0004(3)
SiB	0.4749(1)	0.3373(1)	0.7768(2)	0.0067(3)	0.0076(5)	0.0060(5)	0.0066(4)	−0.0005(3)	−0.0010(3)	0.0000(3)
O1A	0.1853(1)	0.3349(2)	0.0563(4)	0.0085(5)	0.0056(11)	0.0105(12)	0.0093(10)	−0.0010(9)	−0.0004(8)	0.0003(9)
O1B	0.5639(1)	0.3383(2)	0.7808(4)	0.0089(5)	0.0048(11)	0.0130(13)	0.0088(10)	0.0001(9)	−0.0008(8)	0.0001(9)
O2A	0.3103(1)	0.5011(3)	0.0613(4)	0.0097(5)	0.0116(12)	0.0072(11)	0.0103(10)	0.0005(9)	0.0004(9)	−0.0010(10)
O2B	0.4354(1)	0.4903(3)	0.7033(4)	0.0104(5)	0.0114(12)	0.0104(12)	0.0093(10)	0.0020(9)	0.0005(9)	0.0032(9)
O3A	0.3041(1)	0.2310(3)	0.8334(4)	0.0100(5)	0.0092(12)	0.0137(13)	0.0072(9)	−0.0039(9)	0.0005(9)	0.0003(9)
O3B	0.4490(1)	0.2129(3)	0.5638(4)	0.0106(5)	0.0096(12)	0.0140(13)	0.0083(10)	−0.0054(9)	0.0004(9)	−0.0018(9)

B chain (φ_B = 151.92°), which for the majority of orthopyroxenes falls between 136.2 and 144.2° (Cameron and Papike 1981; Cámara et al. 2006) (Fig. 2), except for Zn$_2$Si$_2$O$_6$ orthopyroxene, which has φ_B = 149.2° (Morimoto et al. 1975). In fact, the Li$_{0.52}$Mg$_{0.96}$Sc$_{0.52}$Si$_2$O$_6$ orthopyroxene displays the most extended tetrahedral B chain and, thus, the smallest difference between the kinking angles of the A and B chains ($\varphi_A - \varphi_B$ = 13.48°) of all orthopyroxene structures measured at ambient conditions. Furthermore, our sample represents the first orthopyroxene structure that has a kinking angle of the B chain greater than 150°, one of the critical values that has been used for the topological classifications of pyroxene and other chain silicate structures based on ideal close-packing of O atoms (Thompson 1970; Papike et al. 1973; Pannhorst 1979; Thompson and Downs 2003). In particular, Pannhorst (1979) used the φ value of 150° to distinguish different oxygen-atom layers: a K-layer is defined with $\varphi < 150°$ and an S-layer with $\varphi > 150°$. With this geometrical criterion, Pannhorst (1979) speculated a new structure type, which possesses the same space group (*Pbca*) as orthopyroxene, but an O3-O3-O3 angle of the B chain greater than 150°. Examination of the literature on orthopyroxenes reveals that this new structure type has actually been observed in several Fe-bearing orthopyroxenes at high temperatures (Smyth 1973; Sueno et al. 1984; Yang and Ghose 1995b). Very intriguing is that the B chain (φ_B = 173.1°)

in the (Mg$_{0.75}$Fe$_{0.25}$)$_2$Si$_2$O$_6$ orthopyroxene becomes straighter than the A chain (φ_A = 170.8°) at 1023 °C (Yang and Ghose 1995b), which may be a precursor of a structural transformation to either *Pbcn* protopyroxene or *C*2/*c* high-temperature clinopyroxene. Nevertheless, those high-temperature structures possessing the features of the new structure type predicted by Pannhorst (1979) are unquenchable and invert back to orthopyroxene as temperature decreases. Hence, our sample has demonstrated, for the first time, the stability of such a new structure type at ambient conditions.

The configurational variations of the silicate tetrahedral chains in pyroxenes lead to a different coordination for the neighboring M2 cations, which is rather irregular in many structures. In orthopyroxenes, the M2 cations are generally regarded as bonded to six oxygen atoms (within 3 Å radius) (Downs 2003). With increasing temperature, the number of nearest neighbor O atoms changes from six to seven, and back to six (with a switch of O3B atoms), depending on the extension of the tetrahedral B chain (Cameron and Papike 1981; Yang and Prewitt 2000). Owing to the marked straightening of the B chain in our sample, seven oxygen atoms are within the distance of 3 Å around the M2 cation (Table 2) (Fig. 1), with five M2-O distances being shorter than 2.4 Å and two longer than 2.8 Å, forming a (5 + 2) coordination environment. This coordination is comparable to that in the (Mg$_{0.3}$Fe$_{0.7}$)$_2$Si$_2$O$_6$ orthopyroxene at 700 °C (Smyth 1973) or the (Mg$_{0.75}$Fe$_{0.25}$)$_2$Si$_2$O$_6$ orthopyroxene at 923 °C (Yang and Ghose 1995b). The Zn$_2$Si$_2$O$_6$ orthopyroxene also shows a large φ_B value (149.2°) (Fig. 2), but its M2 cation has a (4 + 2) coordination: four M2-O distances are shorter than 2.05 Å and two longer than 2.69 Å (Morimoto et al. 1975).

Relative to other orthopyroxenes, the apparent straightening of the silicate B chain in our sample is a direct consequence of the substitution of an appreciable amount of trivalent Sc^{3+} (r_{Sc}^{3+} = 0.745 Å) for divalent cations in the M1 site (r_{Mg}^{2+} = 0.72 Å and r_{Fe}^{2+} = 0.78 Å) (Shannon 1976). In the orthopyroxene structure, each M1 octahedron shares two O1A-O1B edges with other M1 octahedra to form zigzag octahedral chains along the *c* axis, to which both tetrahedral A and B chains are linked (Fig. 1). Expectedly, an obvious increase of trivalent cations in the M1 sites will significantly increase the M1-M1 cation repulsion across the shared O1A-O1B edges, confirming the mechanism proposed by Cámara et al. (2006) based on Li-Fe doped orthoestatite. As a result, when compared to Mg$_2$Si$_2$O$_6$ orthoenstatite (Yang and Ghose 1995a; Hugh-Jones and Angel 1994), our sample shows an increase of the M1-M1 separation from 3.097 to 3.196(1) Å, coupled with a reduction of the shared O1A-O1B edge from 2.868 to 2.832(2) Å. Accompanied with these changes is the noticeable extension of the tetrahedral B chain and the *c* dimension, which increases from 5.180(1) Å in orthoenstatite to 5.271(1) Å in our sample. Considering the M1-M1 separation of 3.271 Å in *C*2/*c* LiScSi$_2$O$_6$ clinopyroxene, in which the M1 site is fully occupied by Sc^{3+} (Hawthorne and Grundy 1977), there appears to be a strong correlation between the M1-M1 distance and the Sc^{3+}/Mg^{2+} ratio in the M1 site, regardless of the symmetries of pyroxene structures. The reason why the A chain does not show the "abnormal" behavior, as the B chain does, is attributable to the presence of Li$^+$ in the M2 site. Due to the parity violation in the orthopyroxene structure (Thompson 1970), the tetrahedral A chain is straighter than the B chain and the SiA tetrahedron,
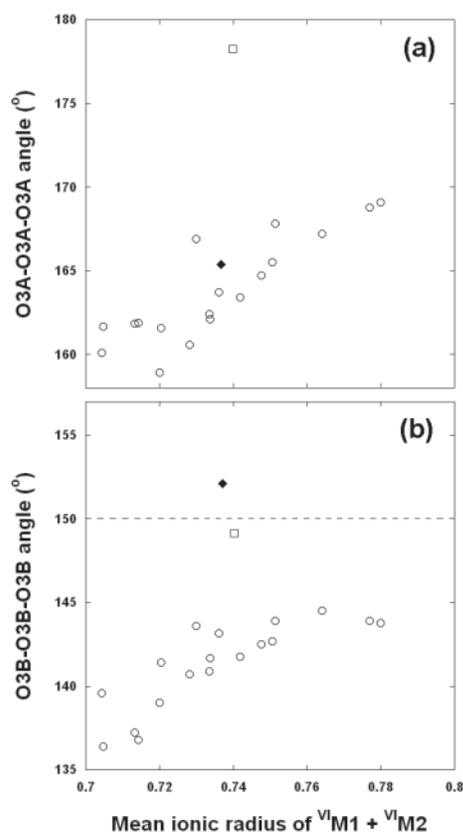
FIGURE 2. Variations of (**a**) the A and (**b**) B chain angles with mean ionic radius of (^{VI}M1 + ^{VI}M2) in *Pbca* orthopyroxenes. Open circles are data taken from Cameron and Papike (1981) and open squares from Morimoto et al. (1975). Our data are indicated by solid diamonds.

which shares the O2A-O3A edge with the M2 polyhedron, is more distorted than the SiB tetrahedron (Cameron and Papike 1981). The replacement of a large amount of divalent cations in the M2 site by monovalent Li$^+$ not only reduces the effective M2 charge valence significantly, but also increases the M2-SiA cation separation from 2.807 Å in orthoestatite to 2.823(1) Å in our sample. Accordingly, the repulsion between M2 and SiA across the shared O2A-O3A edge and, thus, the effects of the parity violation on the tetrahedral A chain are greatly reduced in Li$_{0.52}$Mg$_{0.96}$Sc$_{0.52}$Si$_2$O$_6$ orthopyroxene, offsetting, to a certain extent, the effects of the increased M1-M1 separation on the configurations of silicate chains.

From the structural model of regular tetrahedra and octahedra, Thompson (1970) and Papike et al. (1973) suggested that ideal structural symmetries for protopyroxene and orthopyroxene should be $P2_1cn$ and $P2_1ca$, respectively, rather than the commonly observed $Pbcn$ and $Pbca$. Nonetheless, only one substantiated example for a pyroxene having the symmetry predicted by Thompson (1970) has been reported so far, which was found in Li$_{0.23}$Mg$_{1.54}$Sc$_{0.23}$Si$_2$O$_6$ protopyroxene (Yang et al. 1999). This protopyroxene has the $Pbcn$ space group at ambient conditions and transforms to the $P2_1cn$ symmetry between 2.03 and 2.50 GPa. Based on the structural data for $P2_1cn$ high-pressure protopyroxene, Yang and Prewitt (2000) derived a structure model for the predicted $P2_1ca$ orthopyroxene, which would consist of four symmetrically distinct silicate chains and four nonequivalent metal sites (two for M1 and two for M2). Chemically, our sample appears to be an ideal candidate for the predicted $P2_1ca$ phase, as it has a nearly perfect 1:1 ratio for Mg^{2+} and Sc^{3+} to order into two distinct M1 sites, as well as for Mg^{2+} and Li$^+$ into two different M2 sites. Energetically, the differences in cation size, charge, and electronegativity between Mg^{2+} and Sc^{3+}, as well as between Mg^{2+} and Li$^+$, should also favor the ordered $P2_1ca$ structure. Another composition that may lead to the ordered $P2_1ca$ orthopyroxene structure is (Li$_{0.5}$Mg$_{0.5}$)(Mg$_{0.5}$Al$_{0.5}$)Si$_2$O$_6$. Examples of ordered pyroxene structures resulting from mixed chemical compositions have been observed in (Ca,Na)(Mg,Al)Si$_2$O$_6$ omphacites (Rossi 1988; Rossi et al. 1983) and Na(Mg$_{0.5}$Si$_{0.5}$)Si$_2$O$_6$ clinopyroxene synthesized at 1600 °C and 15 GPa (Angel et al. 1988). Perhaps, a high-pressure environment is required for the formation of the ordered $P2_1ca$ orthopyroxene structure.

REFERENCES CITED

Angel, R.J., Gasparik, T., Ross, N.L., Finger, L.W., Prewitt, C.T., and Hazen, R.M. (1988) A silica-rich sodium pyroxene phase with six-coordinated silicon. Nature, 335, 156–158.
Arlt, T. and Angel, R.J. (2000) Displacive phase transitions in C-centered clinopyroxenes: spodumene, LiScSi$_2$O$_6$ and ZnSiO$_3$. Physics and Chemistry of Minerals, 27, 719–731.
Cámara, F., Iezzi, G., Tiepolo, M., and Oberti, R. (2006) The crystal chemistry of lithium and Fe^{3+} in synthetic orthopyroxene. Physics and Chemistry of Minerals (in press) (DOI: 10.1007/s00269-006-0094-x).
Cameron, M. and Papike, J.J. (1981) Structural and chemical variations in pyroxenes. American Mineralogist, 66, 1–50.
Downs, R.T. (2003) Topology of the pyroxenes as a function of temperature, pressure, and composition as determined from the procrystal electron density. American Mineralogist, 88, 556–566.

Hawthorne, F.C. and Grundy, H.D. (1977) Refinement of the crystal structure of LiScSi$_2$O$_6$ and structure variations in alkali pyroxenes. Canadian Mineralogist, 15, 50–58.
Hugh-Jones, D.A. and Angel, R.J. (1994) A compressional study of MgSiO$_3$ up to 8.5 GPa. American Mineralogist, 79, 405–410.
Ito, J. (1975) High temperature solvent growth of orthoenstatite, MgSiO$_3$: in air. Geophysical Research Letters, 2, 533–536.
Ito, J. and Steele, I.M. (1976) Experimental studies of Li$^+$ + Sc^{3+} coupled substitution in the Mg-silicates: olivine, clinopyroxene, orthopyroxene, protopyroxene, and a new high temperature phase with c = 27 Å. Geological Society of America, Annual Meeting, Denver, Abstracts, 937–938.
Kosoi, A.L., Malkova, L.A., and Frank-Kamenetskii, V.A. (1974) Crystal-chemical characteristics of rhombic pyroxenes. Kristallografya, 19, 282–288.
Morimoto, N., Nakajima, Y., Syono, Y., Akimoto, S., and Matsui, Y. (1975) Crystal structures of pyroxene-type ZnSiO$_3$ and ZnMgSi$_2$O$_6$. Acta Crystallographica, B31, 1041–1049.
Murakami, T., Takéuchi, Y., and Yamanaka, T. (1985) High-temperature crystallography of a protopyroxene. Zeitschrift für Kristallographie, 173, 87–96.
Ohashi, H. and Ii, N. (1978) Structure of CaScAlSiO$_6$ pyroxene. Journal of Mineralogy, Petrology, and Economical Geology, 73, 267–273.
Ohashi, H., Fujita, T., and Ii, N. (1979) Structure of Ca$_{1.00}$Sc$_{0.84}$Ti$_{0.27}$Al$_{1.16}$Si$_{0.73}$O$_6$ pyroxene. Journal of Mineralogy, Petrology, and Economical Geology, 74, 280–286.
Ohashi, H., Osawa, T., Sato, A., and Tsukimura, K. (1996) Crystal structures of (Na,Ca)(Sc,Zn)Si$_2$O$_6$ clinopyroxenes formed at 6 GPa pressure. Journal of Mineralogy, Petrology, and Economical Geology, 91, 21–27.
Pannhorst, W. (1979) Structural relationships between pyroxenes. Neues Jahrbuch für Mineralogie Abhandlungen, 135, 1–17.
Papike, J.J., Prewitt, C.T., Sueno, S., and Cameron, M. (1973) Pyroxenes: compositions of real and ideal structural topologies. Zeitschrift für Kristallographie, 138, 254–273.
Redhammer, G. and Roth, G. (2004a) Structural variation and crystal chemistry of LiMe^{3+}Si$_2$O$_6$ clinopyroxenes Me^{3+} = Al, Ga, Cr, V, Fe, Sc, and In. Zeitschrift für Kristallographie, 219, 278–294.
——— (2004b) Structural changes upon the temperature dependent $C2/c \rightarrow P21/c$ phase transition in LiMe^{3+}Si$_2$O$_6$ clinopyroxenes, Me = Cr, Ga, Fe, V, Sc, and In. Zeitschrift für Kristallographie, 219, 585–605.
Robinson, K., Gibbs, G.V., and Ribbe, P.H. (1971) Quadratic elongation, a quantitative measure of distortion in coordination polyhedra. Science, 172, 567–570.
Rossi, G. (1988) A review of the crystal-chemistry of clinopyroxenes in eclogites and eclogite-facies rocks. In D.C. Smith, Ed., Eclogites and eclogite-facies rocks, p. 237–270. Elsevier, Amsterdam.
Rossi, G., Smith, D.C., Ungaretti, L., and Domeneghetti, C. (1983) Crystal-chemistry and cation ordering in the system diopside-jadeite: A detailed study by crystal structure refinement. Contributions to Mineralogy and Petrology, 83, 247–258.
Sheldrick, G.M. (1997) SHELXS97 and SHELXL97. University of Göttingen, Germany.
Smyth, J.R. (1973) An orthopyroxene structure up to 850 °C. American Mineralogist, 58, 636–648.
Smyth, J.R. and Ito, J. (1977) The synthesis and crystal structure of a magnesium-lithium-scandium protopyroxene. American Mineralogist, 62, 1252–1257.
Shannon, R.D. (1976) Revised effective ionic radii and systematic studies of interatomic distances in halides and chalcogenides. Acta Crystallographica, A32, 751–767.
Sueno, S., Cameron, M., and Prewitt, C.T. (1984) The crystal structure of high clinoferrosilite. American Mineralogist, 61, 38–53.
Takéuchi, Y., Kudoh, Y. and Ito, J. (1984a) New series of superstructures based on a clinopyroxene. I. The structure of the 'enstatite-IV' series, [Mg$_{(x-12)/3}$Sc$_4$][Li$_{4/3}$Si$_{(x-4)/3}$]O$_x$, with x = 100, 112, or 124. Acta Crystallographica, B40, 115–125.
——— (1984b) New series of superstructures based on a clinopyroxene. II. The structure of the Sc series of enstatite-IV, [Mg$_{-(x-7.5)/3}$Sc$_{-3}$][Mg$_{2/3}$Si$_{(x-4)/3}$]O$_x$, with x = 100, 112 or 124. Acta Crystallographica, B40, 126–132.
——— (1984c) New series of superstructures based on a clinopyroxene. III. Higher-order superstructures. Acta Crystallographica, B40, 257–262.
Thompson, J.B., Jr. (1970) Geometrical possibilities for amphibole structures: model biopyriboles. American Mineralogist, 55, 292–293.
Thompson, R.M. and Downs, R.T. (2003) Model pyroxenes: ideal pyroxene topologies. American Mineralogist, 88, 653–666.
Yang, H. and Ghose, S. (1995a) High-temperature single-crystal X-ray diffraction studies of the ortho-proto phase transition in enstatite, Mg$_2$Si$_2$O$_6$, at 1360 K. Physics and Chemistry of Minerals, 22, 300–310.
——— (1995b) A transitional structural state and anomalous Fe-Mg order-disorder in Mg-rich orthopyroxene, (Mg$_{0.75}$Fe$_{0.25}$)$_2$Si$_2$O$_6$. American Mineralogist, 81, 1117–1125.
Yang, H. and Prewitt, C.T. (2000) Chain and layer silicates at high temperatures and pressures. In R.M. Hazen and R.T. Downs, Eds., High-temperature and high-pressure crystal chemistry, 41, p. 211–255. Reviews in Mineralogy and Geochemistry, Mineralogical Society of America, Chantilly, Virginia.
Yang, H., Finger, L.W., Conrad, P.G., Prewitt, C.T., and Hazen, R.M. (1999) High-pressure single-crystal X-ray diffraction and Raman study of the $Pbcn$-$P2_1cn$ phase transition in protopyroxene. American Mineralogist, 84, 245–256.